*Proc. Natl. Acad. Sci. USA*
Vol. 88, pp. 8164–8168, September 1991
Chemistry

# A first-order reaction controls the binding of antigenic peptides to major histocompatibility complex class II molecules

(antigen presentation/kinetics)

STEPHAN N. WITT AND HARDEN M. MCCONNELL*

Stauffer II Laboratory of Physical Chemistry, Stanford University, Stanford, CA 94305

*Contributed by Harden M. McConnell, June 27, 1991*

ABSTRACT **Major histocompatibility complex class II molecules have been reported to bind antigenic peptides very slowly *in vitro*. To investigate the molecular events that govern the slow binding reaction, we have determined the dependence of complex formation and dissociation on peptide concentration. The complex between the purified major histocompatibility complex class II protein I-$E^k$ and a fluoresceinated peptide representing amino acids 89–104 of pigeon cytochrome *c* (FpCyt*c*) was studied. Two important results emerge from this study. (*i*) At pH 5.4, the half-time for I-$E^k$–FpCyt*c* complex formation is equal to ≈7 hr for peptide concentrations that vary over a range of three orders of magnitude. There is in fact a small but significant *decrease* in the half-time for complex formation at *low* peptide concentrations. The small decrease in half-time is related to the release of endogenous peptides. (*ii*) At large ratios of peptide to protein ([FpCyt*c*]/[I-$E^k$] > 40), the half-times for I-$E^k$–FpCyt*c* complex formation and dissociation are equal to one another to within a factor of two between pH 7.5 and 4.5. The present results demonstrate that a slow, first-order reaction precedes complex formation between I-$E^k$ and FpCyt*c*. This first-order reaction may involve a protein conformational change in addition to the release of endogenous peptides.**

Major histocompatibility complex (MHC) class II molecules are polymorphic, heterodimeric membrane-bound proteins that are found on the surfaces of antigen-presenting cells. It is now known that MHC class II molecules bind peptides (1) and display the peptides on the surfaces of antigen-presenting cells for immune surveillance by helper T cells (2). Unlike the fine specificity observed for IgG antibodies, MHC class II proteins are only selective. Each MHC class II molecule can bind many different peptides, with different primary sequences.

Many details of the molecular mechanisms of antigen presentation are incompletely understood. Exogenous antigenic peptides bind to class II molecules with remarkably slow kinetics at pH 7 *in vitro*, over a time scale of days (3). Unfortunately, detailed kinetic studies designed to probe the mechanism of class II–peptide complex formation have been hindered because of low binding of exogenous antigenic peptides to affinity-purified class II molecules. Typically <20% of the binding sites are occupied with added peptides after lengthy incubations. The reported low binding is related to the discovery by Buus *et al.* (4) that up to 90% of the binding sites of purified MHC class II molecules are occupied with endogenous peptides. In the cell, acidic reaction conditions may be essential for the rapid formation of functional I-$A^d$–peptide complexes according to the recent work by Jensen (5) using fixed cells. Jensen showed that complex formation accelerates, and the number of functional complexes increases, at low pH (pH ≈ 5). We find that there is appreciable formation of I-$E^k$–peptide complexes at low pH, whereas there is no detectable formation of complexes at pH ≈7 in detergent solution. Therefore, to investigate the slow kinetics of complex formation, we have undertaken a kinetic study at low pH. We show that the previously reported second-order rate constants for MHC class II–peptide complex formation in detergent solution are inconsistent with the observed formation kinetics (3, 6, 7).

The publication costs of this article were defrayed in part by page charge payment. This article must therefore be hereby marked "*advertisement*" in accordance with 18 U.S.C. §1734 solely to indicate this fact.

## MATERIALS AND METHODS

**Cells and I-$E^k$ Purification.** The B-cell lymphoma CH27 (8), which expresses I-$E^k$ and I-$A^k$, was cultured in RPMI 1640 medium supplemented with 5 mM pyruvate, 10 mM L-glutamine, and 10% Nu-Serum IV (Collaborative Research). I-$E^k$ was isolated by established procedures (9), using the anti-I-$E^k$ monoclonal antibody 14.4.4S (10). Protein concentration was determined by the method of Lowry. For all experiments described in this report, I-$E^k$ was maintained in a buffer consisting of 10 mM sodium phosphate, 150 mM sodium chloride, 0.02% (wt/vol) sodium azide, and 1 mM *n*-dodecyl β-D-maltoside (DM) (Sigma) at pH 7.0. All incubations at low pH were initiated by the addition of an equal volume of citrate buffer of the desired pH (200 mM sodium citrate, 150 mM sodium chloride, and 1 mM DM).

**T-Cell Assay.** I-$E^k$ was reconstituted into lipid vesicles according to the detergent dialysis procedure given by Brian and McConnell (11). A dipalmitoylphosphatidylcholine/dilinoleoylphosphatidylcholine/cholesterol molar ratio of 9:1:2.7 was used (12), with a final lipid-to-protein ratio of 500:1. Lipids were purchased from Sigma. Planar membranes containing I-$E^k$ were incubated with peptide for 24 h and then T cells were added as described (9). After a 24-h incubation with 2B4 cells (13), the supernatants were harvested, subjected to one freeze–thaw cycle, and assayed for interleukin 2 (IL-2) content with the IL-2-dependent cell line HT2 (14). The supernatant was serially diluted, and then HT2 cells were added to a final concentration of $2 \times 10^4$. The total volume was 100 μl. [$^3$H]Thymidine (1 μCi; 1 Ci = 37 GBq; New England Nuclear) was added to each well for the last 16 h of a 40-h incubation (15). Cells were harvested, and the amount of incorporated [$^3$H]thymidine was determined by scintillation counting. The concentration of I-$E^k$ in the vesicle preparation was 53 μg/ml. Controls consisted of identical incubations of planar membranes containing I-$E^k$ without peptides (cpm = 700 ± 200; mean ± SEM) and with a synthetic peptide representing amino acids 323–337 of

Abbreviations: MHC, major histocompatibility complex; pCyt*c*, synthetic peptide representing amino acids 89–104 of pigeon cytochrome *c*; FpCyt*c*, fluorescein-labeled (N terminus) pCyt*c*; HPSEC, high-performance size-exclusion chromatography; DM, dodecyl β-D-maltoside; IL-2, interleukin 2; Ova-(323–337), synthetic peptide representing amino acids 323–337 of chicken ovalbumin.

*To whom reprint requests should be addressed.

chicken ovalbumin [Ova-(323–337)] at 1 μM (cpm = 1000 ± 300; mean ± SEM).

**Peptide Synthesis.** The peptide representing amino acids 89–104 of pigeon cytochrome *c* (pCyt*c*) was synthesized using standard fluoren-9-ylmethoxycarbonyl (F-moc) chemistry. The fluorescently labeled peptide (FpCyt*c*) was prepared by the addition of the succidimidyl ester of 5- (and 6-) carboxyfluorescein (Molecular Probes) directly to the resin after removal of the N-terminal F-moc group. This procedure enabled the selective labeling of the N-terminal amino group. The peptides were purified by using HPLC (semipreparative Vydac $C_{18}$ column). The identity of the labeled and unlabeled peptides was confirmed by mass spectrometry. Fluoresceinated Ova-(323–337) was purchased from Peninsula Laboratories and used without HPLC purification.

**Gel-Filtration Chromatography.** A Pharmacia TSK G3000SW high-performance gel-filtration column (7.5 × 600 mm) with a precolumn (7.5 × 75 mm) was used in the experiments described here. The column run-through went through a Gilson model 121 fluorometer and a standard HPLC absorbance detector set up in series. A 490-nm excitation filter and a 520- to 650-nm emission filter were used to detect the I-$E^k$–FpCyt*c* complexes. The column buffer was typically 50 mM phosphate, 150 mM NaCl, 0.02% (wt/vol) sodium azide, and 1 mM DM at pH 7.0. Standard solutions of 5-carboxyfluorescein (Sigma) were used to estimate the amount of FpCyt*c* bound to I-$E^k$. The flow rate was 1 ml/min.

## RESULTS

In this work we have employed fluorescence-detected, high-performance size-exclusion chromatography (HPSEC) to detect I-$E^k$–FpCyt*c* complexes. Absorbance detection was used simultaneously to monitor the weak absorbance due to the protein at 280 nm. No detectable dissociation of bound peptides occurred during the course of the gel-filtration experiment (15 min) (3).

To identify species eluting from the gel-filtration column, fractions were collected, concentrated, and then subjected to SDS/PAGE under nonreducing conditions (data not shown). The I-$E^k$ heterodimer and the I-$E^k$–FpCyt*c* complex coelute with an elution volume ($V_e$) of 15 ml (Fig. 1, traces B and C). The fraction eluting at 19 ml does not contain protein (Fig. 1, trace A). It is probably due to micelles of the detergent (DM) used in the column experiments, which can trap free fluorescent peptide. When an aliquot of neat column buffer is concentrated and then injected on the HPSEC column, a peak is observed at 19 ml. The intense, broad peak extending from $V_e$ = 24 to 34 ml in the fluorescence-detected chromatograms shown in Fig. 1 is due to free FpCyt*c*.

When the molar ratio of FpCyt*c* to I-$E^k$ ([FpCyt*c*]/[I-$E^k$]) was >10, no significant change in the absorbance intensity of the heterodimer was detected during the course of incubations at 37°C. At the lowest ratio of peptide to protein ([FpCyt*c*]/[I-$E^k$] ≈ 1), there was an approximate 10–20% loss of absorbance from the heterodimers over a period of 50–72 h. The decrease in absorbance at low peptide concentration is the result of either the dissociation of the heterodimers or to nonspecific binding of the heterodimers to the wall of the sample tube (Falcon no. 2058).

**I-$E^k$ Peptide-Binding Capacity vs. pH.** A high level of peptide binding to class II molecules is desired in order to carry out kinetic measurements. To determine if there is augmented binding to affinity-purified I-$E^k$ at low pH, samples of I-$E^k$ were incubated with excess FpCyt*c* at a variety of pH values for ≈3 days. From the fluorescence-detected chromatograms shown in Fig. 1, we estimate that approximately .05%, 2%, 10%, and 0% of the I-$E^k$ binding sites were occupied with FpCyt*c* after 72 h of incubation at pH 7.0, 6.0, 5.0, and 4.0, respectively (Fig. 1). The weak bands at 15 ml

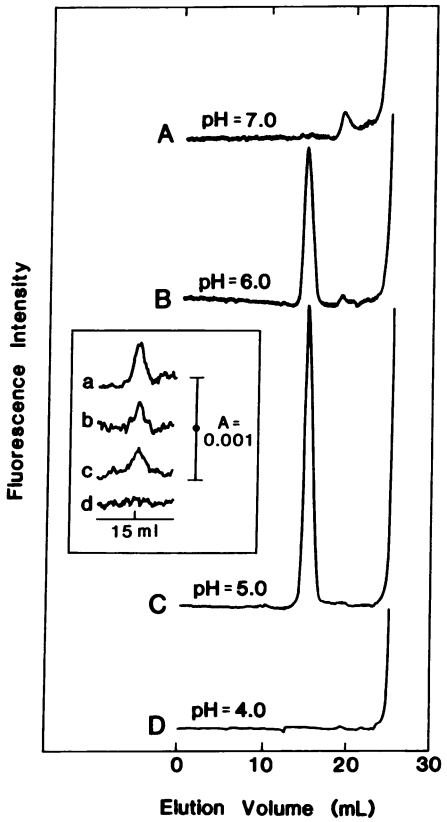


FIG. 1. Fluorescence-detected HPSEC of I-$E^k$–FpCyt*c* complexes. Samples of purified I-$E^k$ were incubated with 10 μM FpCyt*c* for ≈72 h at 37°C. Trace A: pH 7.0, fluorescence sensitivity = 0.01, 200 μl injected. Trace B: pH 6.0, sensitivity = 0.01, 100 μl injected. Trace C: pH 5.0, fluorescence sensitivity = 0.02, 100 μl injected. Trace D: pH 4.0, fluorescence sensitivity = 0.05, 100 μl injected. (*Inset*) The heterodimeric portion of the absorbance-detected chromatograms shows that the protein is not lost during the binding experiments when pH > 4. Traces a–d were obtained from the same samples that traces A–D were obtained from.

in the absorbance-detected chromatograms (Fig. 1 *Inset*) complement the fluorescence data and show that the samples were in the heterodimeric state after the lengthy incubations at pH 7.0, 6.0, and 5.0. In contrast, at pH 4 or less, we observed a complete absence of intensity at 15 ml (Fig. 1 *Inset*), indicating that the heterodimers had dissociated to the free subunits. This latter result agrees with previous work, which demonstrated that the I-$E^k$ heterodimers are unstable at pH ≈ 4–5 and readily dissociate to the free α and β subunits (16). Taken together, the data from the gel-filtration assay show that I-$E^k$ has a bell-shaped binding capacity as a function of pH, with maximum binding at pH 4.5 (Fig. 2).

The biological relevance of the enhanced binding of FpCyt*c* to purified I-$E^k$ at low pH was assessed by performing a functional assay of I-$E^k$ that was reconstituted into planar membranes (9). The results from the T-cell assay confirm that there is an increase in the number of functional complexes produced at acid pH (Fig. 2). Some qualitative differences are evident between the two binding curves: the T-cell assay detected the I-$E^k$–pCyt*c* complex over a wider range of pH than observed in the gel-filtration assay. For example, there is almost no detectable amount of complex at pH 7.0, whereas 25% of the maximum stimulation occurred at pH 7.0 in the T-cell assay (Fig. 2). The maximum in the binding curve from the T-cell stimulation data is also shifted to lower pH (pH = 4.0) relative to the data obtained from gel-filtration assay (pH = 4.5). The cellular assay and the gel-filtration results show the same trend: there is an enhancement in the

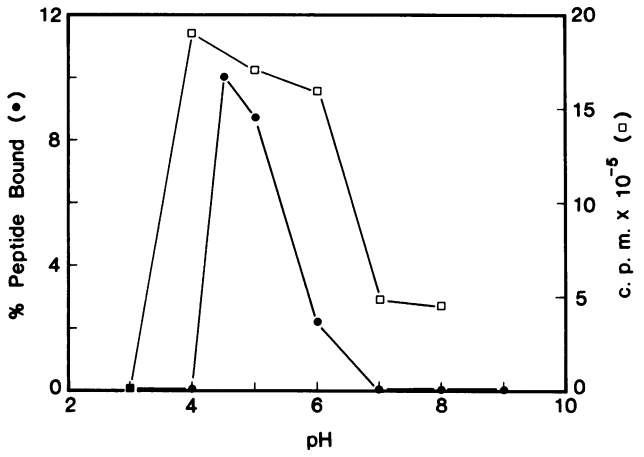


FIG. 2. I-E$^k$ peptide-binding capacity as a function of pH. In the gel-filtration assay, the percentage of I-E$^k$ binding sites occupied after a 72-h incubation with 10 $\mu$M FpCyt*c* at 37°C (●) was determined. The I-E$^k$ concentration was 0.3 $\mu$M. In the T-cell assay, I-E$^k$ was reconstituted into planar membranes and incubated with 1 $\mu$M FpCyt*c* for 24 h at 37°C, at the indicated pH (□). The supernatant was assayed for IL-2 by using the IL-2-dependent cell line HT2.

peptide-binding capacity of purified I-E$^k$ molecules at low pH, with maximal binding at pH 4.0–4.5. These combined results indicate that complexes obtained during our studies on detergent-solubilized class II molecules are the biologically relevant MHC class II–peptide complexes.

**Half-Time of the Association Reaction as a Function of Peptide Concentration.** Class II–peptide complex formation was studied in detail at pH 5.4, since there is appreciable binding at that pH and pH 5.4 approximates the acidity found in endosomes (17). The formation reactions were carried out under pseudo-first-order reaction conditions, where [peptide] >> [I-E$^k$]. If the binding reaction is first order in peptide concentration, the pseudo-first-order rate constant, $k_p$ ($s^{-1}$), is equal to the product of the second-order rate constant, $k_{on}$ ($M^{-1}s^{-1}$) and the peptide concentration. The order of the formation reaction with respect to peptide is determined by varying the peptide concentration under pseudo-first-order reaction conditions. If complex formation is first order in peptide concentration, a plot of $k_p$ vs. [FpCyt*c*] or $t_{1/2}$ vs. 1/[FpCyt*c*] is linear, with the slope equal to $k_{on}$ and ln $2/k_{on}$, respectively. In this report we characterize the formation kinetics in terms of half-times.

The kinetic data obtained from samples with a high molar ratio of FpCyt*c* to I-E$^k$ are nearly superimposable (25 and 200 $\mu$M FpCyt*c*) (Fig. 3). At lower peptide concentrations (2 and 0.2 $\mu$M), where the molar ratio of FpCyt*c* to I-E$^k$ is ≈10 or less, the magnitudes of the initial rates and endpoints are reduced relative to the results obtained at higher peptide concentrations. Each data point shown in Fig. 3 is a ratio of fluorescence intensity to absorbance intensity of all I-E$^k$ complexes at $V_e$ = 15 ml. The value of the asymptote for the sample with 200 $\mu$M peptide is 40 after 64 h of incubation. The endpoints in Fig. 3 correspond to approximately 6%, 5%, and 1% of the I-E$^k$ binding sites occupied with FpCyt*c*.

Complex formation follows first-order kinetics over five half-lives (Fig. 3). The half-times vary from 4 to 11 h ($k_f$ = 4.8 × $10^{-5}$ to 1.8 × $10^{-5}$ $s^{-1}$) and were obtained by fitting the intensity vs. time profiles to an exponential function. The plot of $t_{1/2}$ vs. 1/[FpCyt*c*] (Fig. 3 *Inset*) shows that the half-time for complex formation does not deviate substantially from a value of 7.5 ± 3 h over three orders of magnitude in peptide concentration. The binding reaction is, therefore, zero order in peptide concentration. A significant aspect of the plot of $t_{1/2}$ vs. 1/[FpCyt*c*] is the weak acceleration of the binding reaction as the peptide concentration is lowered from 200 to

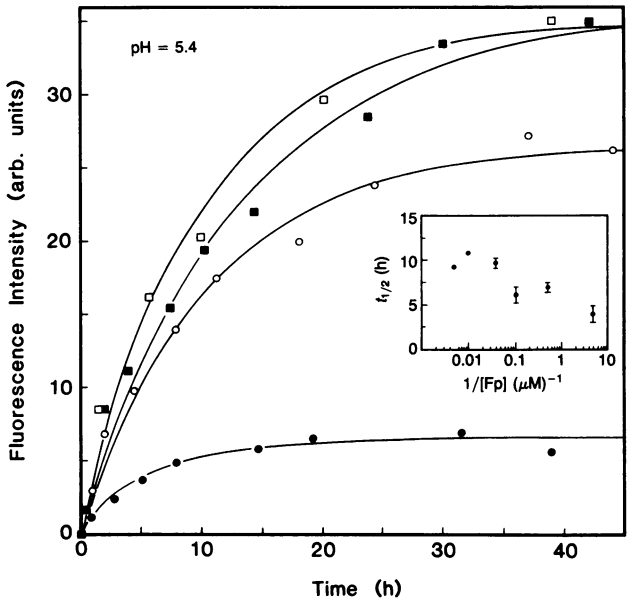


FIG. 3. Kinetics of I-E$^k$–FpCyt*c* complex formation as a function of peptide concentration at pH 5.4. Samples of purified I-E$^k$ were incubated at 37°C with the indicated concentrations of FpCyt*c*, and aliquots were periodically injected to determine the amount of fluorescent complex. The I-E$^k$ concentration was 0.25 $\mu$M. □, 200 $\mu$M FpCyt*c*; ■, 25 $\mu$M FpCyt*c*; ○, 2 $\mu$M FpCyt*c*; ●, 0.2 $\mu$M FpCyt*c*. Data points were fit to an exponential function (solid lines). (*Inset*) Half-time for complex formation vs. 1/[peptide]. Error bars represent the SEM of duplicate samples.

0.2 $\mu$M. This decrease of $t_{1/2}$ for binding at low peptide concentration is discussed below.

**Kinetics of Formation and Dissociation of I-E$^k$–FpCyt*c* Complexes at pH 4.5–7.5.** The half-times for the formation and dissociation of I-E$^k$–FpCyt*c* complexes were determined over a range of pH values (pH 4.5–7.5) to ascertain whether there is a correlation between peptide binding and dissociation. Samples of I-E$^k$ and FpCyt*c* were incubated for up to 3 days at 37°C with excess FpCyt*c* (10 $\mu$M). Periodically, an aliquot of the sample was injected on the HPSEC column to determine the amount of complex that had formed. The fluorescence intensity vs. time profiles shown in Fig. 4 demonstrate that the initial rate of complex formation accelerates as the pH is lowered from physiologic pH and that the amount of FpCyt*c* bound at equilibrium increases at low pH. At pH 7.5, there is no detectable formation of I-E$^k$–FpCyt*c* complexes after 50 h of incubation at 37°C. As shown in Table 1, the half-times for complex formation do not vary significantly when the pH is lowered from pH 6.8 to 5.0. In contrast, there is an ≈3-fold decrease in the half-time from 10.7 h to 2.8 h when the pH is lowered from pH 5.0 to 4.5. The abrupt acceleration in the formation of complexes between pH 5.0 and 4.5 and the increase in the magnitudes of the asymptotes shown in Fig. 4 are consistent with a low pH-induced release of bound self-peptides or a low pH-induced conformational change that results in stronger binding.

Dissociation kinetics of FpCyt*c* from preformed complexes of I-E$^k$–FpCyt*c* were investigated over the same range of pH values. Samples of the complex were prepared by incubating I-E$^k$ with excess FpCyt*c* at pH 5 for 48–72 h at 37°C. After the initial loading period, aliquots were injected on the HPSEC column, and the fraction containing the complex was collected on ice and subsequently concentrated. To initiate the reaction, the sample was mixed with an equal volume of cold citrate buffer of the desired pH, which contained a large molar excess (>1000) of unlabeled pCyt*c*. An aliquot of the cold sample was injected immediately on the HPSEC column to establish the

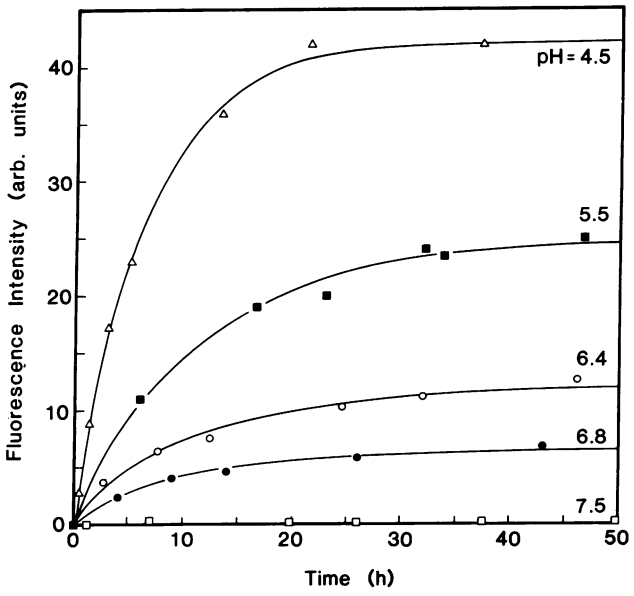


FIG. 4. Kinetics of I-E$^k$–FpCyt*c* complex formation as a function of pH. Samples of purified I-E$^k$ were incubated with excess FpCyt*c* (10 $\mu$M) at 37°C for the indicated times. □, pH 7.5; ●, pH 6.8; ○, pH 6.4; ■, pH 5.5; △, pH 4.5. Data points were fit to an exponential function (solid lines).

initial amount of I-E$^k$–FpCyt*c* complex; the remaining sample was placed in a 37°C incubator. Aliquots were injected at the indicated times to determine the amount of bound FpCyt*c*. A comparison of the half-times for complex formation and dissociation (Table 1) shows that $t_{1/2}$ (on) and $t_{1/2}$ (off) only differ by a factor of two over three orders of magnitude in hydrogen ion concentration. In the experiments described above, the measurements do not distinguish between the loss of $\alpha\beta$FpCyt*c* (where $\alpha$ and $\beta$ represent the subunits of the MHC molecule) signal due to dissociation of FpCyt*c* and dissociation of the complex to form $\alpha$ + $\beta$FpCyt*c* or $\alpha$FpCyt*c* + $\beta$.

## DISCUSSION

This work was undertaken to determine the role of pH and peptide concentration on the kinetics and mechanism of MHC class II–peptide complex formation and dissociation *in vitro*. The quantitative gel-filtration experiments demonstrate that there is a significant enhancement in the peptide-binding capacity of affinity-purified I-E$^k$ at low pH. The augmented binding at low pH was also found with a functional assay. The resultant bell-shaped binding profiles are remarkably similar to those obtained for I-A$^d$ in fixed cells (5). An examination of Fig. 2 shows that the bell-shaped cell stimulation profile from the T-cell assay has a maximum at pH 4, whereas in the gel-filtration assay the maximum in the binding profile occurs at pH 4.5. I-E$^k$ may be more resistant to acid-catalyzed degradation when reconstituted into lipid membranes, a conclusion reached previously (16).

Table 1. Effect of acid on I-E$^k$–FpCyt*c* complex formation and dissociation (37°C)

| | Formation | | Dissociation | |
|---|---|---|---|---|
| pH | $t_{1/2}$ (on), h | $k_f$, $s^{-1}$ × $10^5$ | $t_{1/2}$ (off), h | $k_{off}$, $s^{-1}$ × $10^5$ |
| 7.5 | 0 | 0 | 12.0 | 1.6 |
| 6.8 | 7.4 | 2.6 | — | — |
| 6.0 | — | — | 13.8 | 1.4 |
| 5.5 | 9.6 | 2.0 | 12.0 | 1.6 |
| 5.0 | 10.7 | 1.8 | 8.4 | 2.3 |
| 4.5 | 2.8 | 7 | 5.3 | 3.6 |

Formation reactions were initiated by the addition of an equal volume of citrate buffer, of the desired pH, to the sample of I-E$^k$. FpCyt*c* was immediately added in a minimal volume (10 $\mu$l). Aliquots were periodically injected on the gel-filtration column to determine the amount of complex. Rate constants are the means of duplicates. The standard errors in the values of $k_f$ and $k_{off}$ vary from 0.1 to 0.5 $s^{-1}$ (pH 5.0–7.5). At pH 4.5, where the rate is quite sensitive to pH, the standard errors for $k_f$ and $k_{off}$ are 2 and 0.5 $s^{-1}$, respectively. The dissociation of FpCyt*c* from preformed complexes of I-E$^k$–FpCyt*c* was determined over a range of pH values, in the presence of >1000-fold molar excess of unlabeled pCyt*c*.

The peptide-binding capacity of I-E$^k$ correlates with the dissociation rate constants given in Table 1. The dissociation rate constant ($k_{off}$) increases by a factor of ≈2.5 when the pH is varied from 6.0 to 4.5. Over the same pH range, the observed peptide binding to I-E$^k$ rose from ≈1% to 10%. The binding capacity and $k_{off}$ thus increase in parallel. The enhanced peptide-binding capacity of I-E$^k$ may be due to a low pH acceleration of the dissociation of self-peptides. Specifically, low pH may promote a conformational change in the MHC molecule to a structure that can bind and release peptides. In previous work, low pH has been reported to promote the transition from a "compact" to a "floppy" conformation (16). This latter conformation may be the species that most easily binds and releases peptides.

A series of experiments was designed to probe the mechanism of exogenous peptide binding to MHC class II molecules *in vitro* (Figs. 3 and 4 and Table 1). The experiments in Fig. 3 demonstrate that the half-time for complex formation is not inversely proportional to the peptide concentration, contrary to the assumptions used in previous kinetic studies (3, 6, 7). Therefore, the binding site is either inaccessible [closed conformation (18, 19)] and/or is occupied by self-peptides. In other words, the dominant conformation of the protein does not allow peptide exchange. Table 1 shows that from pH 4.5 to 7.5 $t_{1/2}$ (on) and $t_{1/2}$ (off) differ at most by a factor of two. Based on these two results, we conclude that I-E$^k$–FpCyt*c* complex formation *in vitro* is regulated by a slow, first-order reaction. Similar results have also been obtained using I-A$^d$ and an ovalbumin peptide, indicating that these results are general (20).

Eqs. 1–3 describe a reaction mechanism that is consistent with the observed kinetics. A slow, first-order reaction generates endogenous peptides ($P_s$) and empty MHC molecules (Eq. 1).

$$\alpha\beta\text{–}P_s \underset{k_{on}}{\overset{k_{off}}{\rightleftharpoons}} \alpha\beta + P_s \qquad [1]$$

$$\alpha\beta + \text{FpCyt}c \underset{k_{off}}{\overset{k_{on}}{\rightleftharpoons}} \alpha\beta\text{–FpCyt}c \qquad [2]$$

$$\alpha\beta \xrightarrow{k_3} \alpha + \beta \qquad [3]$$

The empty heterodimers ($\alpha\beta$) bind FpCyt*c* to produce new complexes (Eq. 2) and also rupture, producing $\alpha$ and $\beta$ subunits (Eq. 3). The latter reaction must be very slow in the present experiments. A more rapid cleavage of empty heterodimers causes a significant reduction in the $\alpha\beta$FpCyt*c* signal intensity at long times, as is observed when I-A$^d$ is incubated with fluoresceinated Ova-(323–339) at low pH (20) or when I-E$^k$ is incubated with FpCyt*c* in octyl glucoside at pH 5.2. A loss of signal intensity can also arise from cleavage of $\alpha\beta$FpCyt*c* complexes to generate $\alpha$ + $\beta$FpCyt*c* or $\alpha$FpCyt*c* + $\beta$. The two reactions that cause a loss of $\alpha\beta$FpCyt*c* signal intensity can be distinguished. A large excess of FpCyt*c* ([FpCyt*c*]/[I-Ek] >500) reduces the loss of $\alpha\beta$FpCyt*c* signal intensity, which is otherwise observed when I-E$^k$ is incubated with low concentrations of FpCyt*c* in octyl

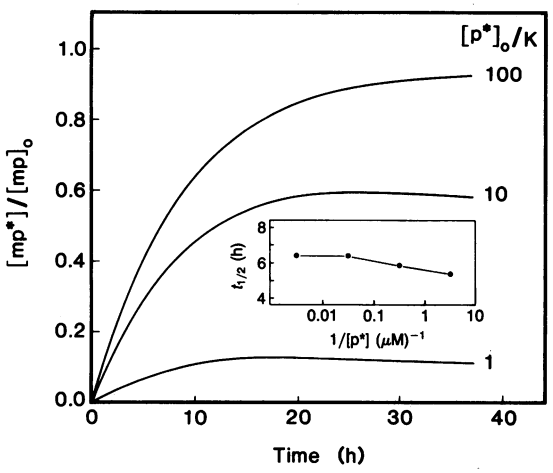


FIG. 5. Simulated formation of fluorescent peptide–class II complexes using the kinetic model in Eqs. 1–3. $[mp^*]/[mp]_0$ is the relative concentration of fluorescent complexes at the indicated ratios of fluorescent peptide $[p^*]_0$ to the equilibrium dissociation constant $K$ ($K = k_{off}/k_{on}$). Conditions: $k_{off} = 3 \times 10^{-5}\ s^{-1}$, $k_{on} = 100\ M^{-1}\ s^{-1}$, $k_3 = 1.5 \times 10^{-5}\ s^{-1}$, $[mp]_0 = 1\ \mu M$. (*Inset*) Half-time for complex formation vs. 1/[peptide].

glucoside at pH 5.2 (unpublished results). According to Eqs. 2 and 3, the rate of empty heterodimer cleavage is inversely related to the peptide concentration.

The calculated formation curves shown in Fig. 5 mimic the experimental curves (Fig. 3) when $k_3/k_{off}$ varies from 0 to 0.5. A plot of calculated formation half-times, obtained from the simulated traces, reveals that $t_{1/2}$ shortens slightly as the peptide concentration is lowered, consistent with the experimental results shown in Fig. 3 *Inset*. Simulations also show that even when $k_3$ is set equal to 0 the half-time for complex formation retains a weak dependence on the peptide concentration. The concentration dependence of $t_{1/2}$ for two consecutive reversible reactions is discussed elsewhere (21).

In conclusion, note that the present kinetic studies relate to the well-known problem of preparing pure MHC–peptide complexes. The prior occupation of the binding sites with self-peptides represents one obstacle to the formation of pure complexes, and the existence of reactive and nonreactive protein conformations such as floppy and compact represent a second potential obstacle. The splitting of the heterodimer into separate $\alpha$ and $\beta$ chains is a third obstacle, since such native chains apparently do not recombine to form the $\alpha\beta$ heterodimer under the conditions of our experiments (22).

We thank Dr. Dan Denney for a critical reading of the manuscript. During this work, S.N.W. was supported by Damon Runyon–Walter Winchell Cancer Fund Fellowship DRG-968 and by National Institutes of Health Grant 5R01 AI13587-13.

1. Livingstone, A. L. & Fathman, C. G. (1987) *Annu. Rev. Immunol.* **5**, 477–540.
2. Schwartz, R. H. (1985) *Annu. Rev. Immunol.* **3**, 237–261.
3. Buus, S., Sette, A., Colon, S. M., Jenis, D. M. & Grey, H. M. (1986) *Cell* **47**, 1071–1077.
4. Buus, S., Sette, A., Colon, S. M. & Grey, H. M. (1988) *Science* **242**, 1045–1047.
5. Jensen, P. E. (1990) *J. Exp. Med.* **171**, 1779–1784.
6. Roche, P. A. & Cresswell, P. (1990) *J. Immunol.* **144**, 1849–1856.
7. Roof, R. W., Luescher, I. F. & Unanue, E. R. (1990) *Proc. Natl. Acad. Sci. USA* **87**, 1735–1739.
8. Haughton, G., Arnold, L. W., Bishop, G. A. & Mercolino, T. J. (1986) *Immunol. Rev.* **93**, 35–51.
9. Watts, T. H., Brian, A. A., Kappler, J. W., Marrack, P. & McConnell, H. M. (1984) *Proc. Natl. Acad. Sci. USA* **81**, 7564–7568.
10. Ozato, T., Mayer, N. & Sachs, D. (1980) *J. Immunol.* **124**, 533–540.
11. Brian, A. A. & McConnell, H. M. (1984) *Proc. Natl. Acad. Sci. USA* **81**, 6159–6163.
12. Quill, H., Carlson, L., Fox, B. S., Weinstein, J. N. & Schwartz, R. H. (1987) *J. Immunol. Methods* **98**, 29–41.
13. Samuelson, L. E., Germain, R. N. & Schwartz, R. M. (1983) *Proc. Natl. Acad. Sci. USA* **80**, 6972–6976.
14. Watson, J. (1979) *J. Exp. Med.* **150**, 1510–1519.
15. Jensen, P. E. (1989) *J. Immunol.* **143**, 420–425.
16. Dornmair, K., Rothenhausler, B. & McConnell, H. M. (1989) *Cold Spring Harbor Symp. Quant. Biol.* **54**, 409–416.
17. Mellman, I., Fuchs, R. & Helenius, H. (1986) *Annu. Rev. Biochem.* **55**, 663–700.
18. Guillet, J.-G., Lai, M.-Z., Briner, T. J., Buus, S., Sette, A., Grey, H. M., Smith, J. A. & Gefter, M. L. (1987) *Science* **235**, 865–870.
19. Schwartz, R. H. (1987) *Nature (London)* **326**, 738–739.
20. Tampé, R. & McConnell, H. M. (1991) *Proc. Natl. Acad. Sci. USA* **88**, 4661–4665.
21. Fersht, A. (1985) *Enzyme Structure and Mechanism* (Freeman, New York), pp. 136–141.
22. Dornmair, K. & McConnell, H. M. (1990) *Proc. Natl. Acad. Sci. USA* **87**, 4134–4138.